

LHC and B physics probes of neutrinoless double beta decay in supersymmetry without R-parity

B. C. Allanach¹, C. H. Kom^{1,2}, H. Päs³

¹ *DAMTP, University of Cambridge, Wilberforce Road, Cambridge, CB3 0WA, UK*

² *Cavendish Laboratory, J.J. Thomson Avenue, Cambridge CB3 0HE, UK*

³ *Fakultät für Physik, Technische Universität Dortmund, D-44221, Dortmund, Germany*

E-mails: b.c.allanach@damp.cam.ac.uk, kom@hep.phy.cam.ac.uk,
heinrich.paes@uni-dortmund.de

ABSTRACT: In the event of an observation of neutrinoless double beta decay, a relevant question would be: what lepton number violating physics is responsible for the decay? The exchange of Majorana neutrinos and/or supersymmetric particles may contribute. We point out that measurements of supersymmetric signals at the LHC, including single slepton production, could be used to help bound some supersymmetric processes contributing to neutrinoless double beta decay. LHC information about the supersymmetric spectrum could be combined with $B_d^0\text{-}\bar{B}_d^0$ mixing data in order to bound a competing neutrinoless double beta decay process involving sbottom exchange.

KEYWORDS: Supersymmetry Phenomenology, Neutrino Physics, B-Physics, Collider Physics.

Contents

1. Introduction	1
2. Mechanisms of $0\nu\beta\beta$ in the RPV MSSM	3
3. Experimental limits	6
4. B_d^0-\bar{B}_d^0 mixing, single slepton production at the LHC and $0\nu\beta\beta$	8
4.1 Implications of $\lambda'_{113}\lambda'_{131}$ bound from B_d^0 - \bar{B}_d^0 on $0\nu\beta\beta$	8
4.2 Single selectron production at the LHC via λ'_{111}	11
5. Discussion and summary	15
A. Parton Level Contributions to $0\nu\beta\beta$	17
A.1 Light Majorana neutrino exchange: $0\nu\beta\beta$ via $m_{\beta\beta}$	17
A.2 Heavy sbottom exchange: $0\nu\beta\beta$ via $\lambda'_{113}\lambda'_{131}$	17
A.3 Sparticle exchange: $0\nu\beta\beta$ via $\lambda'_{111}\lambda'_{111}$	18
B. Nuclear Matrix Elements	19

1. Introduction

Neutrinoless double beta decay ($0\nu\beta\beta$) provides the most sensitive probe of lepton number violation as well as a Majorana nature of neutrinos. At the quark level, $0\nu\beta\beta$ corresponds to the simultaneous transition of two down quarks into two up-quarks and two electrons. While the most prominent mechanism in the literature that causes this decay involves the exchange of a massive Majorana neutrino, several other possibilities have been discussed. Here, we focus on the attractive alternative where $0\nu\beta\beta$ is mediated by the exchange of sparticles in supersymmetric models with R-parity violation [1–5].

R-parity violating couplings arise in a general supersymmetric extension of the Standard Model (SM), where the superpotential contains renormalisable baryon- and lepton-number violating operators. The presence of both sets of operators typically leads to violation of stringent bounds on proton decay [6], unless the parameters are unnaturally suppressed. Proton decay bounds are evaded if a discrete symmetry is imposed which forbids at least one set of such parameters. A widely-studied example is R-parity [7], under which both sets of operators are odd under the parity transformation and hence are forbidden. This symmetry also has the advantage of having the lightest supersymmetric particle (LSP) as a natural dark matter (DM) candidate. On the other hand, there exist R-parity conserving (RPC) dimension 5 operators which could potentially lead to fast proton decay [8, 9]. One way to suppress these operators is by instead imposing proton hexality [11, 12].

Instead of R-parity, we focus on an alternative, namely baryon triality (also known as baryon parity in some literature) [10, 13]. This \mathbf{Z}_3 discrete symmetry allows for the dimension 4 R-parity violating (RPV) terms which violate lepton number, while those that

violate baryon number are forbidden. A significant advantage of this class of models is that dimension 5 proton decay operators are forbidden. The LSP will decay via the non-zero RPV couplings present, hence a neutralino LSP cannot be a dark matter candidate. Other dark matter candidates are viable, for example the gravitino, since its decay is slow on cosmological time scales [14]. Alternatively the dark matter could originate from a hidden sector. In the rest of this paper, we use the term R-parity violation to denote the lepton number violating, R-parity violating interactions. A survey of effective lepton number violating operators may be found for example in [15].

After imposing a symmetry that forbids baryon-number violating terms, the RPV superpotential is

$$\mathcal{W}_{RPV} = \frac{1}{2}\lambda_{ijk}L_iL_j\bar{E}_k + \lambda'_{ijk}L_iQ_j\bar{D}_k - \mu_iL_iH_u, \quad (1.1)$$

where we have suppressed all gauge indices and used the notation of Ref. [16]. The $\{i, j, k\} \in \{1, 2, 3\}$ are family indices. $\lambda_{ijk}, \lambda'_{ijk}$ are dimensionless trilinear RPV couplings, and μ_i are bi-linear RPV parameters, having dimensions of mass.

Compared with the RPC minimal supersymmetric extension to the Standard Model (RPC MSSM), the presence of additional RPV couplings leads to distinctive signatures at a collider and have interesting physical consequences, for example providing neutrino masses. As the RPV couplings violate lepton number by 1 and involve lepton doublets, they automatically lead to Majorana neutrino masses [17–25] without the need to introduce additional field content such as a right handed neutrino. $0\nu\beta\beta$ proceeds through the ‘1-1’ entry in the neutrino Majorana mass matrix $m_{\beta\beta}$ which connects two electron neutrinos in a basis where the charged lepton mass matrix is diagonal. We refer to this mechanism as $m_{\beta\beta}$ contribution in the remainder of the paper. For three left-handed Majorana neutrino masses m_i , with PMNS mixing matrix $U_{\alpha i}$, where $\alpha \in \{e, \mu, \tau\}$ and $i \in \{1, 2, 3\}$,

$$m_{\beta\beta} = \sum_{i=1}^3 m_i U_{ei}^2. \quad (1.2)$$

$m_{\beta\beta}$ may be a complex quantity. There are additional higher dimensional effective operators, characteristic of this class of models, which mediate $0\nu\beta\beta$ without an $m_{\beta\beta}$ insertion. As these operators violate lepton number by two units without the need of an $m_{\beta\beta}$ insertion, they are not suppressed by the smallness of the neutrino masses as a result. These channels will be called *direct contributions*. In general, the direct and $m_{\beta\beta}$ contributions contribute to $0\nu\beta\beta$ simultaneously, so depending on their relative magnitudes, interference between the direct and $m_{\beta\beta}$ decay matrix elements may need to be included in determining the decay rate of $0\nu\beta\beta$.

A measurement of the $0\nu\beta\beta$ rate alone does not fix a neutrino mass scale, since it is possible that direct contributions are non-negligible. However, the RPV couplings leading to the direct contributions can affect other observables, which could then be used to constrain the amplitude of the direct contributions. If they can be experimentally bounded, one may infer $m_{\beta\beta}$ from the $0\nu\beta\beta$ decay rate.

The aim of this paper is to explore the interplay between direct and $m_{\beta\beta}$ contributions, in particular how different constraints and observations may shed light on the underlying mechanisms of $0\nu\beta\beta$. We will show how the combined knowledge of the masses of the electron sneutrino and sbottoms and constraints from $B_d^0-\bar{B}_d^0$ mixing could allow us to determine an upper bound on a direct $0\nu\beta\beta$ channel involving sbottoms. Searches for single slepton production at the LHC could provide valuable information on the value of λ'_{111} , which (with measurements of various sparticle masses) will allow one to bound its direct contribution to $0\nu\beta\beta$. A first exploration on the relationship between $0\nu\beta\beta$ decay rate and single slepton production at the LHC may be found in [26]. A complementary way to probe mechanisms of $0\nu\beta\beta$ was discussed in [27, 28] by combining measurements from different nuclei. Efforts to relate neutrino masses and collider phenomenology in other theories with lepton number violation may be found for instance in [29].

For concreteness, we only consider $0\nu\beta\beta$ of ^{76}Ge . In the rest of this paper, numerical values of nuclear matrix elements (NMEs) and half life all refer to this nucleus. A related work on contributions of trilinear RPV terms to $0\nu\beta\beta$ is presented in [30]. There, particular attention is paid to nuclear matrix element calculations and contributions from different sparticles in the presence of a non-zero λ'_{111} coupling. We go beyond the scope of this work in several ways: most importantly, we focus on what may be inferred from different experimental measurements on the mechanism that produces $0\nu\beta\beta$. We have also corrected certain terms in the effective Lagrangian at the quark level, that were incorrect in the literature.

This paper is organised as follows. In section 2 we briefly review the possible $0\nu\beta\beta$ mechanisms in the RPV MSSM. The current experimental half life limit $T_{1/2}^{0\nu\beta\beta}$ of ^{76}Ge , as well as the neutrino oscillation data are summarised in section 3. We also list some useful scaling relations between the RPV parameter bounds and SUSY breaking parameters used there. In section 4.1 we proceed to discuss how the RPV contribution to $B_d^0-\bar{B}_d^0$ mixing can affect the possibility of the $\lambda'_{113}\lambda'_{131}$ direct contribution to be the dominant observable $0\nu\beta\beta$ channel. We then investigate the prospects of observing the single selectron resonance at the LHC and its implication of $0\nu\beta\beta$ in section 4.2, before concluding in section 5. Technical information about parton-level $0\nu\beta\beta$ calculations is in Appendix A and our NMEs are listed in Appendix B.

2. Mechanisms of $0\nu\beta\beta$ in the RPV MSSM

In the RPV MSSM, it is possible to construct Majorana neutrino mass models that explain the neutrino oscillation data [13, 21, 25, 31–36]. $0\nu\beta\beta$ could proceed through standard light Majorana neutrino exchange with the $m_{\beta\beta}$ mass insertion. In addition, there are direct contributions via the RPV coupling products $\lambda'_{113}\lambda'_{131}$ and $\lambda'_{111}\lambda'_{111}$.

The RPV coupling products $\lambda'_{ilm}\lambda'_{jml}$ contribute to the neutrino mass matrix $(m_\nu)_{ij}$, in particular they generate the ‘1-1’ entry $m_{\beta\beta}$. A Feynman diagram using the mass insertion approximation (MIA) [37] with $\lambda'_{113}\lambda'_{131}$ is shown in fig. 1. In this approximation, $m_{\beta\beta}$ can

be written as

$$m_{\beta\beta} \simeq \frac{3m_d}{8\pi^2} \frac{\lambda'_{113}\lambda'_{131}m_{bLR}^2}{m_{bLL}^2 - m_{bRR}^2} \ln\left(\frac{m_{bLL}^2}{m_{bRR}^2}\right) + (b \leftrightarrow d). \quad (2.1)$$

Here m_{bLL}^2 , m_{bRR}^2 and m_{bLR}^2 represent the entries of the sbottom mass matrix in an obvious notation, and m_d is the running mass of the down quark. $0\nu\beta\beta$ may then proceed via exchange of a virtual Majorana neutrino with a $m_{\beta\beta}$ insertion. A Feynman diagram depicting this process is displayed in fig. 2. For a realistic model, one expects there to be many non-vanishing bi-linear and/or tri-linear RPV operators present in order to fill out the effective 3×3 neutrino mass matrix with non-zero entries. Bi-linear RPV couplings could also lead to direct $0\nu\beta\beta$. However, as discussed in [39], neutrino mass terms obtained from these couplings that are consistent with the observed neutrino mass scales typically lead to negligible direct contributions to the $0\nu\beta\beta$ rate. On this basis we neglect their direct contribution, but bear in mind the possibility that they may enhance $m_{\beta\beta}$ beyond what is expected from the tri-linear couplings. We also expect that the λ_{ijk} couplings may contribute to $m_{\beta\beta}$, but not to affect direct $0\nu\beta\beta$ significantly. Coupling products of the form $\lambda'_{11k}\lambda'_{ik1}$ and $\lambda'_{k11}\lambda_{i1k}$ could violate lepton number i and electron number by 1 unit each. For $i \neq 1$, their contributions to direct $0\nu\beta\beta$ via PMNS mixing are suppressed by the mass scale of the light neutrinos. As a result their contributions to direct $0\nu\beta\beta$ is likely to be subdominant and will not be discussed further in this paper.

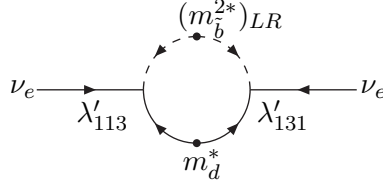


Figure 1: An example diagram showing a contribution to $m_{\beta\beta}$ from the product $\lambda'_{113}\lambda'_{131}$.

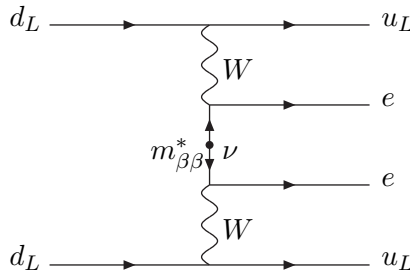


Figure 2: A Feynman diagram showing $0\nu\beta\beta$ via exchange of a virtual Majorana neutrino.

A Feynman diagram representing a direct contribution mediated by $\lambda'_{113}\lambda'_{131}$ is shown in fig. 3. As the corresponding matrix element does not contain neutrino mass insertions, it is not suppressed by the smallness of the neutrino mass scale. In principle, the product

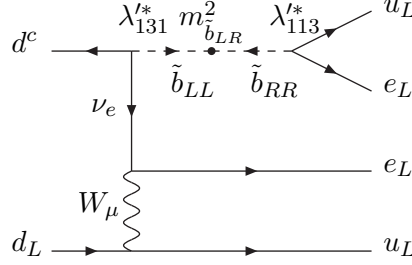


Figure 3: Direct $\lambda'_{113}\lambda'_{131}$ contribution to $0\nu\beta\beta$.

$\lambda'_{112}\lambda'_{121}$ could also lead to $0\nu\beta\beta$. However, this coupling product is tightly constrained by $K^0-\bar{K}^0$ mixing [38], and hence this contribution is neglected in the rest of this paper.

It should be noted that $\lambda'_{111}\lambda'_{111}$ can also mediate $0\nu\beta\beta$ via a diagram similar to fig. 3. However, in the case of $\lambda'_{111}\lambda'_{111}$, there are other diagrams contributing to $0\nu\beta\beta$ which dominate. These diagrams are shown in fig. 4.

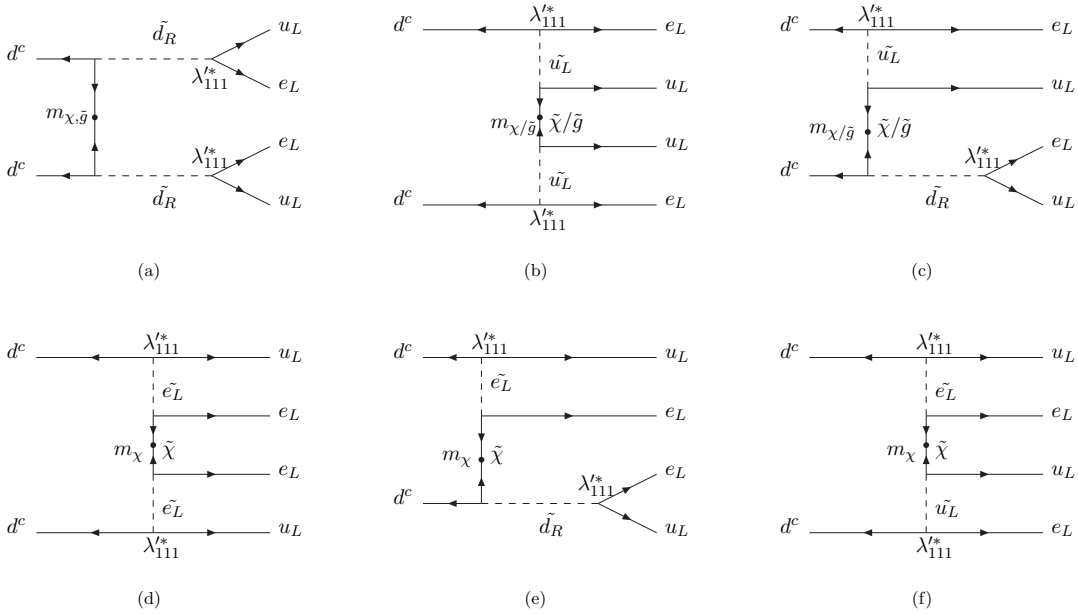


Figure 4: $\lambda'_{111}\lambda'_{111}$ contributions to $0\nu\beta\beta$.

3. Experimental limits

The most stringent lower limit on the ^{76}Ge $0\nu\beta\beta$ half life was bounded by the Heidelberg-Moscow experiment [40, 41] to be

$$T_{1/2}^{0\nu\beta\beta} \geq 1.9 \cdot 10^{25} \text{ yrs.} \quad (3.1)$$

The most common interpretation of such a limit is in terms of a model in which only $m_{\beta\beta}$ contributes to $0\nu\beta\beta$. In the event of an observation in the next round of $0\nu\beta\beta$ searches, the half-life will be used to infer $|m_{\beta\beta}|$, as in fig. 5. The figure shows that in the event of an observation of $T_{1/2}^{0\nu\beta\beta} < 10^{27}$ years, $|m_{\beta\beta}| > 50$ meV. $|m_{\beta\beta}| \gtrsim 10$ meV implies a non-hierarchical (i.e. inverted or quasi-degenerate) spectrum [42].

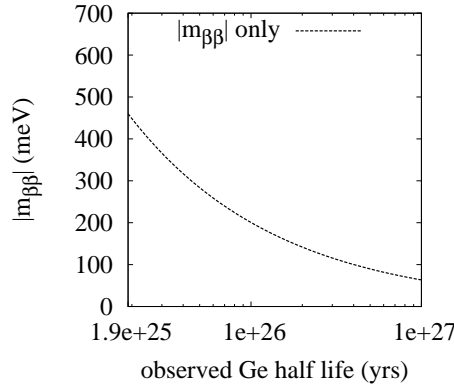


Figure 5: Value of $m_{\beta\beta}$ inferred from a future observation of $T_{1/2}^{0\nu\beta\beta}$, for our NMEs and assuming only Majorana neutrino exchange contributes.

Such inferences depend crucially on the assumption that no other process (for example, direct RPV processes) contribute to $0\nu\beta\beta$. We shall now take into account the possibility that the direct RPV processes can simultaneously contribute to $m_{\beta\beta}$. Depending on the RPV couplings considered, different mechanisms dominate the $0\nu\beta\beta$ process. Thus eq. (3.1) can be translated to upper bounds on particular products of RPV couplings. For the model under consideration, the relevant formula is given by

$$(T_{1/2}^{0\nu\beta\beta})^{-1} = G_{01} |M_{tot}|^2 = G_{01} \left| \frac{m_{\beta\beta}}{m_e} M_\nu + e^{i\phi_1} |M_{\lambda'_{113}\lambda'_{131}}| + e^{i\phi_2} |M_{\lambda'_{111}}| \right|^2, \quad (3.2)$$

where $G_{01} = 7.93 \cdot 10^{-15} \text{ yr}^{-1}$ [43] is a precisely calculable phase space factor and $e^{i\phi_{1,2}}$ are relative complex phases between the various contributions. These matrix elements represent contributions from the direct ($M_{\lambda'_{111}}, M_{\lambda'_{113}\lambda'_{131}}$) and the neutrino mass (M_ν) mechanisms.

If $m_{\beta\beta}$ is the dominant contribution to $0\nu\beta\beta$, using the value of M_ν displayed in Appendix B, the bound in eq. (3.1) can be translated into the limit

$$m_{\beta\beta} \lesssim 460 \text{ meV.} \quad (3.3)$$

If instead the direct contributions are dominant, then assuming the $m_{\beta\beta}$ contributions are negligible, eq. (3.1) leads to [1, 2, 4, 5]

$$\lambda'_{113}\lambda'_{131} \lesssim 2 \cdot 10^{-8} \left(\frac{\Lambda_{SUSY}}{100\text{GeV}} \right)^3, \quad (3.4)$$

$$\lambda'_{111} \lesssim 5 \cdot 10^{-4} \left(\frac{m_{\tilde{f}}}{100\text{GeV}} \right)^2 \left(\frac{m_{\tilde{g}/\tilde{\chi}}}{100\text{GeV}} \right)^{1/2}, \quad (3.5)$$

respectively, after taking into account the modifications to the effective Lagrangians discussed in Appendix A. Here Λ_{SUSY} is an effective SUSY breaking scale for the soft terms involved in eq. (A.3), and $m_{\tilde{f}}$ and $m_{\tilde{g}/\tilde{\chi}}$ are sfermions and gluino/neutralino masses in the dominant Feynman diagrams.

Clearly, the bounds on the RPV couplings depend on the SUSY mass spectra. We thus make a simple assumption about the RPC soft SUSY breaking terms: that they follow the minimal supergravity (mSUGRA) boundary conditions. The resulting SUSY mass spectra are obtained using the spectrum generator **SOFTSUSY** [16]. At the SUSY scale, all RPV couplings are set to zero except for either λ'_{111} or λ'_{113} and λ'_{131} . This allows us to emphasise effects from the above RPV couplings, without additional complications. Specifically, the following set of parameters are defined:

$$M_0 = [40, 1000] \text{ GeV}, \quad M_{1/2} = [40, 1000] \text{ GeV}, \quad A_0 = 0, \quad \tan\beta = 10, \quad \text{sgn}\mu = +1, \quad (3.6)$$

where M_0 , $M_{1/2}$ and A_0 are the universal scalar, gaugino, and trilinear soft SUSY breaking parameters defined at a unification scale $M_X \sim 2.0 \cdot 10^{16} \text{ GeV}$, $\tan\beta$ is the ratio of the Higgs vacuum expectation values v_u/v_d , and $\text{sgn}\mu$ is the sign of the bi-linear Higgs parameter in the superpotential.

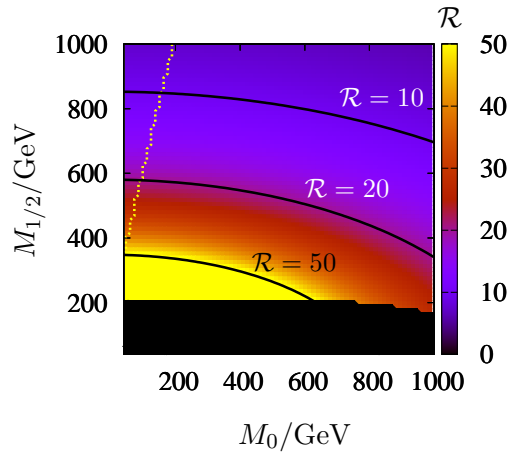


Figure 6: Ratio $\mathcal{R} = |M_{\lambda'_{113}\lambda'_{131}}/M_{m_{\beta\beta}}|$, where $M_{m_{\beta\beta}} = (m_{\beta\beta}/m_e)M_\nu$, in RPV contributions to neutrinoless double beta decay. The blacked region out at the bottom of the plot is excluded and the dotted line delimits regions of different LSP (see text).

We now turn to interference between different contributions to the $0\nu\beta\beta$ rate and discuss first the case where both $m_{\beta\beta}$ and a direct RPV contribution are due to the same

product of RPV couplings. In previous studies, such interference was neglected. For direct contributions, this is a good approximation for a SUSY mass scale Λ_{SUSY} of the order 100 GeV, as the $m_{\beta\beta}$ generated from the same RPV couplings is sub-dominant. However, for fixed RPV couplings, $M_{\lambda'_{111}}$ scales as $\Lambda_{\text{SUSY}}^{-5}$, $M_{\lambda'_{113}\lambda'_{131}}$ scales as $\Lambda_{\text{SUSY}}^{-3}$, whereas $m_{\beta\beta}$ scales as $\Lambda_{\text{SUSY}}^{-1}$. Thus the $m_{\beta\beta}$ contribution would dominate at high SUSY breaking scales. The ratio $\mathcal{R} = |M_{\lambda'_{113}\lambda'_{131}}/M_{m_{\beta\beta}}|$, where $M_{m_{\beta\beta}} = (m_{\beta\beta}/m_e)M_\nu$ is shown in fig. 6. The region in black at low $M_{1/2}$ has either no electroweak symmetry breaking (EWSB), and/or the lightest Higgs mass is in violation of the LEP2 direct search limits [44]. The LEP2 95% confidence level upper bound implies $m_h > 114.4$ GeV, but we impose $m_h > 111.4$ GeV in order to include a 3 GeV theory uncertainty in the `SOFTSUSY` prediction of m_h . The yellow dotted line on the left separates the region with a stau (left) and a neutralino (right) LSP. We see that while in the lower mass region the direct contributions dominate over the $m_{\beta\beta}$ contributions, they become comparable in the high mass region, where interference cannot be neglected. We thus include interference terms in the calculations which follow.

On the other hand, despite the $\Lambda_{\text{SUSY}}^{-5}$ dependence on $M_{\lambda'_{111}}$, the ratio $|M_{\lambda'_{111}}/M_{m_{\beta\beta}}|$ is greater than 20 in our parameter space region. This is because $m_{\beta\beta}$ generated by λ'_{111} is heavily suppressed by the running up quark mass insertions in the loop diagrams. For this reason, we may safely neglect $m_{\beta\beta}$ contributions to $0\nu\beta\beta$ when considering cases with non-zero λ'_{111} unless it originates from some other coupling.

4. $B_d^0-\bar{B}_d^0$ mixing, single slepton production at the LHC and $0\nu\beta\beta$

4.1 Implications of $\lambda'_{113}\lambda'_{131}$ bound from $B_d^0-\bar{B}_d^0$ on $0\nu\beta\beta$

It was shown in [4] that for sparticle masses of ~ 100 GeV, a stringent bound on $\lambda'_{113}\lambda'_{131}$ comes from $0\nu\beta\beta$. Another competing bound comes from $B_d^0-\bar{B}_d^0$ mixing. A Feynman diagram of the latter process is displayed in fig. 7. A recent update [45] by the CKMfitter

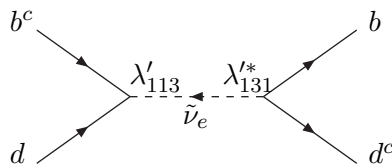


Figure 7: $B_d^0-\bar{B}_d^0$ mixing through coupling product $\lambda'_{113}\lambda'_{131}$.

group shows that at 95% confidence level, the magnitude of any new physics effect to $B_d^0-\bar{B}_d^0$ mixing must be less than the SM contribution. This result is shown in fig. 8. In this figure, the Standard Model solution is located at $\Delta_d = 1$, and deviation from unity represents new physics effects contributing to $B_d^0-\bar{B}_d^0$ mixing. The upper limit of $\lambda'_{113}\lambda'_{131}$ is obtained by updating the results in [4] to take into account the latest $B_d^0-\bar{B}_d^0$ mixing data. We obtain

$$\lambda'_{113}\lambda'_{131} \leq 4.0 \cdot 10^{-8} \frac{m_{\tilde{\nu}_e}^2}{(100\text{GeV})^2}. \quad (4.1)$$

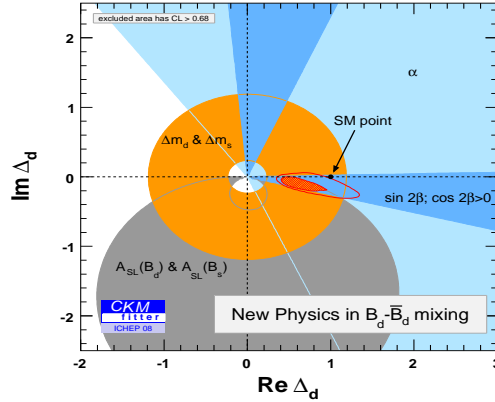


Figure 8: Possible new physics contributions to $B_d^0-\bar{B}_d^0$, from Ref. [66]. The 95% C.L. region is shown in solid orange line. The SM solution is located at $\Delta_d = 1$, and deviation from the SM value may be attributed to the RPV contributions proportional to $\lambda'_{113}\lambda'_{131}$.

To compare limits on $\lambda'_{113}\lambda'_{131}$ from $B_d^0-\bar{B}_d^0$ and from $0\nu\beta\beta$, we recall that the bound from $0\nu\beta\beta$ depends on the sbottom mass squared matrix. In the case where all SUSY breaking parameters are of the same order of magnitude, this bound relaxes approximately as the cube of the sbottom mass scale, which is more rapid compared with the $B_d^0-\bar{B}_d^0$ bound in eq. (4.1). However in the most general MSSM the mass parameters relevant for these two bounds are independent. Which of the bounds is more stringent depends therefore on the ratio of sneutrino to sbottom masses.

In the following, we restrict our discussion to the parameter space discussed in section 3. From [4], we expect the $0\nu\beta\beta$ bound to be more stringent only in very low Λ_{SUSY} of around 100 GeV. With the new $B_d^0-\bar{B}_d^0$ limit, and the fact that mSUGRA-like mass spectra generally have squarks much heavier than the sleptons, we find that the bound from $B_d^0-\bar{B}_d^0$ mixing is more stringent than that from $0\nu\beta\beta$ in all allowed regions of parameter space we explore. This means that if the direct $\lambda'_{113}\lambda'_{131}$ contribution is the only source of $0\nu\beta\beta$, then $T_{1/2}^{0\nu\beta\beta}$ must be larger than the current experimental limit. This conclusion is sensitive to theoretical uncertainties in our predicted value of $T_{1/2}^{0\nu\beta\beta}$ coming from the NMEs. Estimates in such uncertainties vary: NME calculations based on different nuclear model assumptions and input parameters could differ by a factor of 1.3, 3 or even up to 5 [64, 65]. These are then squared in order to obtain the half-life prediction. We take for example a factor of 3 uncertainty in the predicted half life, equivalent to ± 0.5 in $\log_{10} T_{1/2}^{0\nu\beta\beta}$. If the NMEs predicted $T_{1/2}^{0\nu\beta\beta}$ to be a factor of 3 less than the values taken here, then there is a small region where the stronger bound would instead originate from $T_{1/2}^{0\nu\beta\beta}$ at the lowest viable values of $M_{1/2}$ and $M_0/\text{GeV} \sim 400 - 600$. See the appendix for details about the NMEs.

The variation of the $T_{1/2}^{0\nu\beta\beta}$ lower limit, obtained from an upper bound on $\lambda'_{113}\lambda'_{131}$ from $B_d^0-\bar{B}_d^0$ mixing is shown in fig. 9. As in fig. 6, the (blue) dotted line separates regions with stau LSP and neutralino LSP, while the black region at the bottom is excluded due to no

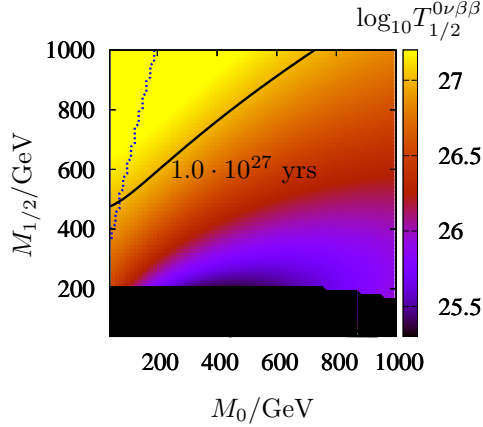


Figure 9: Lower limit on $T_{1/2}^{0\nu\beta\beta}$ (^{76}Ge), using upper limit on $\lambda'_{113}\lambda'_{131}$ obtained from $B_d^0-\bar{B}_d^0$ mixing. The black contour shows where a $T_{1/2}^{0\nu\beta\beta}$ limit of 10^{27} yrs is expected. The black region at the bottom of the plot is excluded and the dotted line delimits regions of different LSP (see text).

EWSB or the higgs being too light. We see that $T_{1/2}^{0\nu\beta\beta} \sim 10^{26}-10^{27}$ yrs is still allowed in much of the parameter space, so that $0\nu\beta\beta$ can be detected by next generation experiments. In particular, there exist good prospects of observing a $0\nu\beta\beta$ signal in the region with relatively low $M_{1/2}$. This is because the sbottom masses receive large renormalisation effects from the gluino mass and as a result are much lighter in the low $M_{1/2}$ region. This in turn enhances $M_{\lambda'_{113}\lambda'_{131}}$ compared with corresponding values in the high $M_{1/2}$ region.

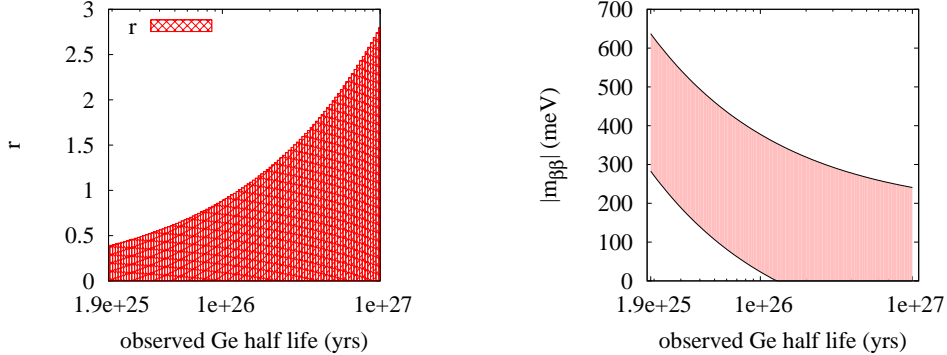


Figure 10: Effect of a near-future measurement of $T_{1/2}^{0\nu\beta\beta}$ for $M_0 = 680$ GeV, $M_{1/2} = 440$ GeV, given current $B_d^0-\bar{B}_d^0$ mixing constraints. In both panels, the shaded regions are allowed.

We now consider the case where sbottom exchange plus other possible processes contribute to $0\nu\beta\beta$, and where $m_{\beta\beta}$ may not be solely due to $\lambda'_{131}\lambda'_{113} \neq 0$ leading to the process in fig. 1. Thus, we consider that there may be other contributions to $m_{\beta\beta}$, coming from bi-linear RPV couplings, or λ_{ijk} couplings, for example. We imagine that LHC measurements are compatible with lepton-number violating mSUGRA signals, with $M_0 = 680$ GeV and $M_{1/2} = 440$ GeV, $A_0 = 0$ and $\tan\beta = 10$. In practice, these numbers would

be determined with some uncertainties, which we ignore for now since we are merely illustrating the point. Then, a measurement of $T_{1/2}^{0\nu\beta\beta}$ in the next generation of experiments could constrain the $0\nu\beta\beta$ mechanism when combined with $B_d^0-\bar{B}_d^0$ constraints. In order to quantify how much of the $0\nu\beta\beta$ width may come from direct processes involving sbottoms, we define

$$r = \left| \frac{M_{\lambda'_{113}\lambda'_{131}}}{M_{tot}} \right|, \quad (4.2)$$

where M_{tot} is the total matrix element including both sbottom mediated and $m_{\beta\beta}$ -induced contributions. $r = 1$ implies that the sbottom-mediated contributions could account for all of the $0\nu\beta\beta$, whereas $r < 1$ requires some extra component (for example from $m_{\beta\beta}$). $r > 1$ also requires an additional component that destructively interferes with the sbottom exchange process. We illustrate this in fig. 10, where the hatched region in the left-hand panel shows which values of r would be allowed by current $B_d^0-\bar{B}_d^0$ mixing constraints. We see that, for $T_{1/2}^{0\nu\beta\beta} < 10^{26}$ years, it is not possible to explain $0\nu\beta\beta$ with sbottom exchange while simultaneously satisfying $B_d^0-\bar{B}_d^0$ bounds. The right-hand panel shows what the inferred value of $m_{\beta\beta}$ may be assuming that the only contributions are from sbottom exchange and $m_{\beta\beta}$. The range of values comes from the possible size of the direct sbottom-mediated contributions and the fact that the interference could be either constructive or destructive. We again see that $T_{1/2}^{0\nu\beta\beta} < 10^{26}$ years would imply that the direct contribution may not account for $0\nu\beta\beta$ alone. Theoretical uncertainties in the $T_{1/2}^{0\nu\beta\beta}$ predictions coming from NMEs would affect the inferences in fig. 10, widening the band in the right-hand panel and raising the bound in the left-hand panel.

4.2 Single selectron production at the LHC via λ'_{111}

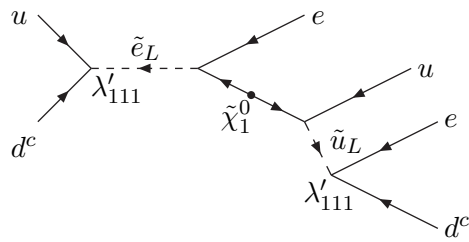


Figure 11: Production of a single selectron at resonance via λ'_{111} , followed by a gauge decay into an electron with a neutralino LSP. The LSP further decays into three final states via a virtual sparticle, leading to a same sign, di-lepton signal for the whole resonance production process.

Depending on the value of λ'_{111} , resonant production of a single selectron may be observed at the LHC. The related process of single smuon production is studied in [46] where like sign di-lepton signals are used because of small backgrounds. A diagram showing like sign di-lepton production, with decay of a selectron via a neutralino is displayed in fig. 11. Earlier studies based on different signatures can be found in [47–51]. For previous analyses

of lepton number violation utilizing the same sign di-lepton signature see e.g. [52–55]. A first study of single slepton production in stau LSP scenarios can be found in [56]. However, to the best of our knowledge, the discovery reach of such stau LSP scenarios at the LHC is not available in the literature, and hence our following discussion will be restricted to the case with a neutralino LSP.

At low sparticle mass scales of ~ 100 GeV, the stringent bound from $0\nu\beta\beta$ renders single slepton production unobservable. However the strong dependence of this bound on the SUSY mass scale, as shown in eq. (3.5), means that it may be possible for this process to be observed at higher SUSY mass scales.

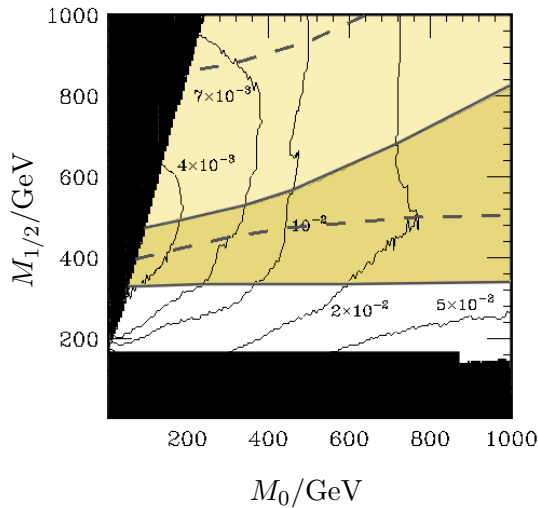


Figure 12: mSUGRA parameter space in which single slepton production may be observed at the LHC for $m_{\beta\beta} = 0$, $\tan\beta = 10$, $A_0 = 0$ and 10fb^{-1} of integrated luminosity at 14 TeV centre of mass energy. In the top left-hand black triangle, the stau is the LSP, a case not covered by this analysis. The bottom black region is ruled out by direct search constraints. The labelled contours are extracted from Ref. [46], and show the search reach given by the labelled value of λ'_{111} . From bottom to top, the white, dark-shaded and light-shaded regions show that observation of single slepton production at the 5σ level would imply $T_{1/2}^{0\nu\beta\beta} < 1.9 \cdot 10^{25}\text{yrs}$, $100 > T_{1/2}^{0\nu\beta\beta}/10^{25}\text{yrs} > 1.9$ and $T_{1/2}^{0\nu\beta\beta} > 1 \cdot 10^{27}\text{yrs}$, respectively. The upper and lower dashed curves show where the contour between the dark-shaded and light-shaded regions would move to if $|m_{\beta\beta}| = 0.05$ eV were included with constructive or destructive interference, respectively.

We will now compare the discovery reach of λ'_{211} [46] at the LHC via single smuon production with the bounds on λ'_{111} coming from $0\nu\beta\beta$. As Ref. [46] does not include detector effects, the reach of λ'_{211} is expected to be readily applicable to λ'_{111} without significant changes. For this reason we shall use the discovery reach of λ'_{211} interchangeably with that of λ'_{111} from now on and use the results of Ref. [46] as an estimate of the 5σ -significance discovery reach for 10fb^{-1} of LHC integrated luminosity at a centre of mass energy of 14 TeV. Cuts were placed on the leptons: a minimum transverse energy cut and an isolation cut in order to reduce heavy quark backgrounds. Other SUSY processes are

cut by requiring a maximum missing transverse energy and requiring that there are at most 2 or 3 jets above a minimum transverse momentum. We refer the interested reader to Ref. [46] for more details.

Fig. 12 shows regions of the $M_0 - M_{1/2}$ plane where single slepton production may be observed via like-sign electrons plus two jets. The black regions with high $M_{1/2}$ and low M_0 have a stau LSP. As discussed before, this is not included in our discussion because a detailed Monte Carlo study is not yet available (however see [56] for an initial study). The black regions with small $M_{1/2}$ are excluded as in fig. 3. In the white region, single slepton production by λ'_{111} could not be observed without violating the current bound upon $T_{1/2}^{0\nu\beta\beta}$. The darker shaded region shows where the observation of single slepton production at 5σ above background implies that $0\nu\beta\beta$ is within the reach of the next generation of experiments, which should be able to probe $T_{1/2}^{0\nu\beta\beta} < 1 \times 10^{27}$ yrs [57, 58]. Conversely, if $0\nu\beta\beta$ is discovered by the next generation of experiments, we should expect single slepton production to be observable and test the λ'_{111} hypothesis. We do not expect A_0 or $\tan\beta$ to affect the shape of the regions much, since they have a negligible effect on the selectron mass and the couplings in the relevant Feynman diagrams. In the light shaded (upper) region, a 5σ single slepton discovery at the LHC implies that the next generation of experiments would not be able to observe $0\nu\beta\beta$. Conversely, if $0\nu\beta\beta$ is within reach of the next generation of experiments, the LHC would see single slepton production signal in this region at greater than 5σ significance.

If $0\nu\beta\beta$ is marginally observed at the limit of the next round of $0\nu\beta\beta$ experiments, it is possible that a contribution from $m_{\beta\beta}$ could contribute significantly (if it originated from a different coupling to λ'_{111}). For ^{76}Ge , a reach of $T_{1/2}^{0\nu\beta\beta} \sim 10^{27}$ yrs implies that an inverted or quasi-degenerate neutrino mass spectrum may contribute to $0\nu\beta\beta$ at an observable level. Whether it interferes with the direct contribution amplitude constructively or not will affect the potential observability at the LHC, and should be taken into account. We shall assume that $|m_{\beta\beta}| = \sqrt{\Delta m_{atm}^2} \sim 0.05$ eV, as implied by neutrino oscillation data. We show in fig. 12 where the upper edge of the darker region would move to and constructive (upper dashed curve) or destructive (lower dashed curve) interference between the $m_{\beta\beta}$ contribution and the direct contributions. We see that for the case of constructive interference in fig. 12, discovery of single slepton production becomes very difficult with 10fb^{-1} of data. On the other hand, the situation improves substantially if destructive interference occurs instead. To see this, we note that for a fixed $T_{1/2}^{0\nu\beta\beta}$, the introduction of a non-vanishing $m_{\beta\beta}$ which interferes destructively with $M\lambda'_{111}$ would imply an increase in the direct contributions. This would require an increase in λ'_{111} , or a decrease in the mass of the SUSY spectrum, or both, all of which lead to an increase in single slepton production rate. We see that single selectron production may be observed for $M_{1/2} \gtrsim 500$ GeV. If the neutrino mass spectrum is instead normal hierarchical, the $m_{\beta\beta}$ diagram will be sub-dominant for the half life discussed above. This situation may be approximated by setting $m_{\beta\beta} = 0$.

We show in fig. 13 the variation of the discovery reach of λ'_{111} with M_0 along the line $M_{1/2} = 300\text{ GeV} + 0.6M_0$. Above the dotted light line, single slepton production will be observed at the LHC. We see from the figure that for nearly all of the parameter

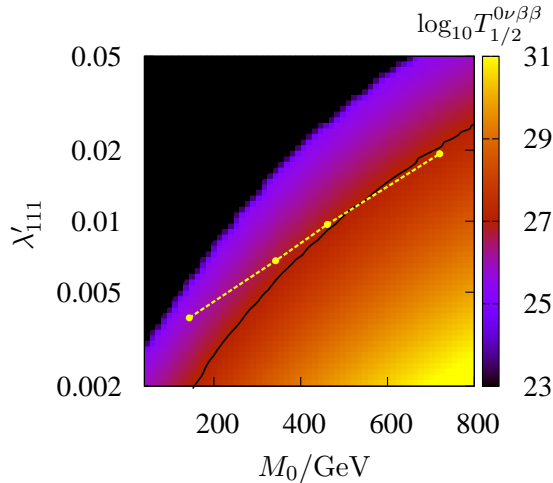


Figure 13: Comparison of $T_{1/2}^{0\nu\beta\beta}$ and single slepton discovery reach as a function of λ'_{111} along the mSUGRA slope $M_{1/2} = 300 \text{ GeV} + 0.6M_0$, with $A_0 = 0$, $\tan\beta = 10$ and $\text{sgn}\mu = 1$. The black region on the top left corner is ruled out by $0\nu\beta\beta$. The region above the solid black line is accessible in near future $0\nu\beta\beta$ experiments, whereas the light dotted line shows the lower limit of λ'_{111} for single slepton production to be discoverable at the LHC.

space where $0\nu\beta\beta$ can be measured by the next generation of experiments, the LHC would provide a confirmation of the supersymmetric origin of the signal by observing single slepton production at the 5σ level.

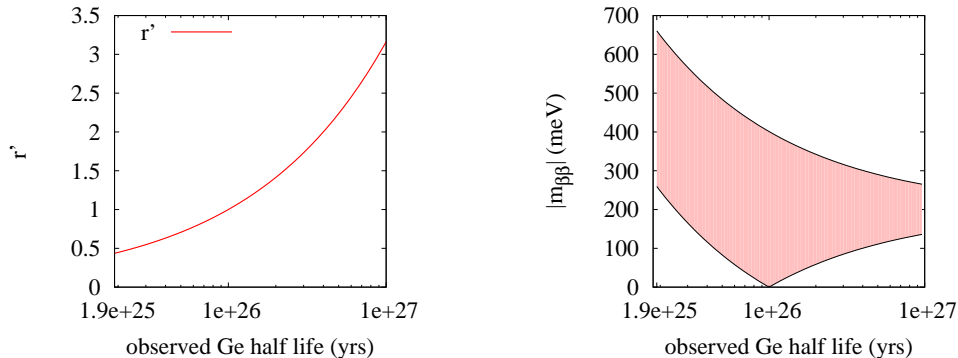


Figure 14: Effect of a near-future measurement of $T_{1/2}^{0\nu\beta\beta}$ for $M_0 = 680 \text{ GeV}$, $M_{1/2} = 440 \text{ GeV}$, given a 5σ observation of single slepton production at the LHC in 10 fb^{-1} at 14 TeV centre of mass energy. In the right-hand panel, the shaded region would be allowed.

We now ask the question: if single slepton production were observed at the LHC, and a measurement of $T_{1/2}^{0\nu\beta\beta}$ were made, what could be divined about the relative contributions

between direct or Majorana neutrino-induced $0\nu\beta\beta$? We define

$$r' = \left| \frac{M_{\lambda'_{111}}}{M_{tot}} \right|, \quad (4.3)$$

where M_{tot} is the total matrix element including both sbottom mediated and $m_{\beta\beta}$ -induced contributions. At our parameter test point of $M_0 = 680$ GeV, $M_{1/2} = 440$ GeV, $A_0 = 0$ and $\tan\beta = 10$, a measurement of the single slepton production cross-section could be used to infer a value of λ'_{111} , which would then imply a value of r' . Here, we assume that the cross-section was just at the 5σ level above background and show which r' could be inferred from the measured value of $T_{1/2}^{0\nu\beta\beta}$ in the left-hand panel of fig. 14. The figure shows a definite prediction for r' , which is 1 at a half-life of 10^{26} years, where $0\nu\beta\beta$ could come entirely from the direct contribution. In general, $r' > 1$ requires destructive interference between the λ'_{111} contribution and another contribution (either $\lambda'_{131}\lambda'_{113}$ or $m_{\beta\beta}$). Assuming the relative phases between different contributions are real, in the destructive interference case there are two solutions to $|M_{\lambda'_{111}} - M_{other}| = |M_{tot}|$, where $|M_{tot}|$ is a prescribed constant derived from $T_{1/2}^{0\nu\beta\beta}$ and eq. (3.2). We note that NME uncertainties, which are neglected here, would turn the definite prediction into a band of possible predictions. The r' prediction would acquire error bands, at the level of $\sim \mathcal{O}(20)\%$, from measurement errors in the SUSY spectrum, cross-section and NME uncertainties. A further dedicated study including simulations of the experiments is required in order to quantify these latter errors more exactly.

The right-hand panel of fig. 14 shows correspondingly what may be deduced about $m_{\beta\beta}$, also neglecting measurement and NME errors, but taking into account two possible contributions to the matrix element: M_ν and $M_{\lambda'_{111}}$. If instead we assumed that $0\nu\beta\beta$ was due entirely to the Majorana neutrino induced contribution, then one deduces $m_{\beta\beta}$ from $T_{1/2}^{0\nu\beta\beta}$ as in fig. 5. We see that the definite prediction widens to a band, due to the relative complex phase between the two contributions to the matrix element. Any inferred value $m_{\beta\beta} \gtrsim 10$ meV corresponds to a non-hierarchical pattern (i.e. inverted or quasi-degenerate) of neutrino masses, and so one would infer that the hierarchy is non-hierarchical for $T_{1/2}^{0\nu\beta\beta} \gtrsim 10^{27}$ years. We see that, for this parameter space point, if $T_{1/2}^{0\nu\beta\beta} \approx 10^{26}$ years, the observation of single slepton would imply that a normal hierarchy is still viable, although still one could not tell without additional measurements if the neutrino mass hierarchy were inverted or hierarchical. On the other hand, for $T_{1/2}^{0\nu\beta\beta} > 1.1 \times 10^{26}$ years or $T_{1/2}^{0\nu\beta\beta} < 0.9 \times 10^{26}$ years, neutrino masses have the non-hierarchical pattern. It remains to be seen how large this window remains after measurement uncertainties are calculated. In the limit where the contributions from $m_{\beta\beta}$ and $M_{\lambda'_{111}}$ are real, a given $T_{1/2}^{0\nu\beta\beta}$ would result in two-fold possible predictions: either the top or the bottom of the bands in the right-hand panel of fig. 14. Theoretical errors originating from the NME calculations would widen the band further.

5. Discussion and summary

In this paper, we have discussed the interplay between a number of observables in RPV

SUSY: $0\nu\beta\beta$, $B_d^0\text{-}\bar{B}_d^0$ mixing and first generation single slepton production at the LHC. We saw that, while it is difficult to infer unambiguously the presence of RPV effects from individual observables, further insight could be gained if these information are analysed simultaneously. Bounds from $B_d^0\text{-}\bar{B}_d^0$ mixing and single slepton production could constrain the extent to which $\lambda'_{113}\lambda'_{131}$ and $\lambda'_{111}\lambda'_{111}$ operators may contribute to $0\nu\beta\beta$. They provide extra handles to complement other strategies for divining the underlying $0\nu\beta\beta$ mechanisms, for example by comparing life times of different nuclei [27].

There are a couple of caveats one should bear in mind however. Firstly, our numerical inference between collider observables and $0\nu\beta\beta$ depends on the relation between the masses of the SUSY particles that mediate the different processes. Constraints on these masses from experiment are required: ideally directly, but otherwise because some other simple theoretical SUSY breaking ansatz such as mSUGRA fits LHC data well. Secondly, the estimated $T_{1/2}^{0\nu\beta\beta}$ is subject to uncertainties in the NME. This is important particularly when using $B_d^0\text{-}\bar{B}_d^0$ data because the sensitivity of the next round of ^{76}Ge $0\nu\beta\beta$ experiments is not expected to go far beyond the 10^{27} yrs level. The bounds from $0\nu\beta\beta$ and $B_d^0\text{-}\bar{B}_d^0$ are comparable in regions with 0.1–1 TeV scale SUSY breaking, with the latter being slightly more stringent in the parameter space we explored. An increase in the NME value used might change this observation.

At present, $B_d^0\text{-}\bar{B}_d^0$ mixing implies only an upper bound on the possible contribution of heavy sbottom exchange to any measurement of $T_{1/2}^{0\nu\beta\beta}$, given information on the SUSY spectrum from the LHC. Sbottom exchange could be solely responsible for $T_{1/2}^{0\nu\beta\beta}(^{76}\text{Ge})$ of $\sim 10^{26}$ yrs, which is potentially observable in the near future. However, the measured value of $T_{1/2}^{0\nu\beta\beta}$ could still require there to be a non-zero Majorana neutrino contribution, depending upon its value. A much more informative two-sided bound on the sbottom exchange contribution would result if a future measurement of $B_d^0\text{-}\bar{B}_d^0$ mixing required an extra component from outside the Standard Model.

We point out that, contrary to previous expectations, a same sign di-lepton signal from single selectron production via gauge decay at the LHC could be observed. This is despite the stringent bound from $0\nu\beta\beta$, because the constraint from $0\nu\beta\beta$ on λ'_{111} relaxes rapidly as the SUSY scale increases. We have shown that if a direct contribution via λ'_{111} is the dominant $0\nu\beta\beta$ mechanism and $0\nu\beta\beta$ of ^{76}Ge is just beyond the current reach, there is a good chance of observing single selectron production at the LHC. Such a scenario is not ruled out by current $0\nu\beta\beta$ bounds for a heavy enough SUSY spectrum. Knowledge of the SUSY spectrum can be combined with $0\nu\beta\beta$ and single-selectron data to bound the λ'_{111} contribution to $0\nu\beta\beta$. Thus, evidence for other contributions may be obtained (for example from Majorana neutrino exchange) and the size of the other contributions bounded. Under the hypothesis that only the λ'_{111} and $m_{\beta\beta}$ contributions are significant, $m_{\beta\beta}$ may be deduced and information about the neutrino mass spectrum is thus obtained. For some ranges of $T_{1/2}^{0\nu\beta\beta}$, this could settle the question of whether the neutrino spectrum were hierarchical or not without the inclusion of other observables.

It will be an interesting exercise in future work to examine a particular point in parameter space with a dedicated LHC simulation study in order to quantify the errors obtained

on the inferred contributions to $0\nu\beta\beta$ in a combined fit.

Acknowledgments

This work has been partially supported by STFC. We thank the Cambridge SUSY working group, G. Hiller, M. Hirsch and R. Mohapatra for useful conversations. CHK is funded by a Hutchison Whampoa Dorothy Hodgkin Postgraduate Award. HP was partially funded by the EU project ILIAS N6 WP1. BCA and CHK also thank the Technische Universität Dortmund, and HP thanks the University of Cambridge for hospitality offered while part of this work was carried out. Some of the hospitality extended to BCA arose from a Gambrinus Fellowship awarded by the Technische Universität Dortmund.

A. Parton Level Contributions to $0\nu\beta\beta$

A.1 Light Majorana neutrino exchange: $0\nu\beta\beta$ via $m_{\beta\beta}$

The effective Lagrangian after integrating out the W gauge boson, and the $\Delta L_e = 2$ Lagrangian with a virtual Majorana neutrino are

$$\begin{aligned}\mathcal{L}_{EW}^{eff}(x) &= -\frac{G_F}{\sqrt{2}} \left[\bar{e}\gamma^\mu(1-\gamma_5)\nu \bar{u}_y\gamma_\mu(1-\gamma_5)d^y \right], \\ \mathcal{L}_{EW}^{eff, \Delta L_e=2}(x) &= \frac{G_F^2}{2} \left[\bar{e}\gamma_\mu(1-\gamma_5)\frac{m_{\beta\beta}}{q^2}\gamma_\nu e^c \right] \left[J_{V-A}^\mu J_{V-A}^\nu \right],\end{aligned}\quad (\text{A.1})$$

respectively. y is a colour index, and in the second line of eq. (A.1), $J_{V-A}^\mu = \bar{u}_y\gamma^\mu(1-\gamma_5)d^y$. A Feynman diagram depicting this process is displayed in fig. 2.

A.2 Heavy sbottom exchange: $0\nu\beta\beta$ via $\lambda'_{113}\lambda'_{131}$

In the basis where both the down-type quark and the charged lepton mass matrices are diagonal, the coupling product $\lambda'_{113}\lambda'_{131}$ leads to an effective Lagrangian involving exchange of one SUSY particle of the form

$$\begin{aligned}\mathcal{L}_{\lambda'_{113}\lambda'_{131}}^{eff}(x) &= \frac{G_F}{8\sqrt{2}}\eta^n (U_{PMNS}^*)_{ni} \left[\frac{1}{2}(\bar{\nu}_i\sigma^{\mu\nu}(1+\gamma_5)e^c)(\bar{u}_y\sigma_{\mu\nu}(1+\gamma_5)d^y) \right. \\ &\quad \left. + 2(\bar{\nu}_i(1+\gamma_5)e^c)(\bar{u}_z(1+\gamma_5)d^z) \right],\end{aligned}\quad (\text{A.2})$$

where [59]¹

$$\begin{aligned}\eta^n &= \sum_k \frac{\lambda'_{1mk}\lambda'_{nk1}(U_{CKM})_{1m}\sin 2\theta_{\bar{d}_k}}{2\sqrt{2}G_F} \left(\frac{1}{m_{\bar{d}_{k(1)}}^2} - \frac{1}{m_{\bar{d}_{k(2)}}^2} \right) \\ &\simeq -\frac{\lambda'_{113}\lambda'_{n31}}{\sqrt{2}G_F} \left(\frac{m_{\bar{b}_{LR}}^2}{m_{\bar{b}_{LL}}^2 m_{\bar{b}_{RR}}^2 - m_{\bar{b}_{LR}}^4} \right).\end{aligned}\quad (\text{A.3})$$

¹The first term in eq. (A.2) differs from [4, 5] and also the preprint version of [59] by a factor of $\frac{1}{2}$. Our check agrees with the published version of the latter reference.

In eq. (A.2), U_{PMNS} is the 3×3 unitary PMNS neutrino mixing matrix [60, 61], and $\sigma^{\mu\nu} = \frac{i}{2}[\gamma^\mu, \gamma^\nu]$. In eq. (A.3), U_{CKM} is the CKM matrix and $m_{\tilde{d}_k(LL)}^2$, $m_{\tilde{d}_k(LR)}^2$ and $m_{\tilde{d}_k(RR)}^2$ denote entries in the k -th generation down type squark mass squared matrix. In particular, $m_{\tilde{b}_1}$ and $m_{\tilde{b}_2}$ denote the 2 sbottom mass eigenvalues, and $\theta_{\tilde{b}}$ is the sbottom left-right mixing angle. The relations between the mixing angle and the entries in the mass and flavour basis sbottom mass matrices follow those in SOFTSUSY [16].

The complete $0\nu\beta\beta$ matrix element with a leptonic current coupled to a quark current via a W boson does not contain a neutrino mass insertion, and hence is not suppressed by the light neutrino mass scale. The $\Delta L_e = 2$ Lagrangian is given by

$$\begin{aligned} \mathcal{L}_{EW+\lambda'_{113}\lambda'_{131}}^{eff, \Delta L_e=2}(x) &= \frac{G_F^2}{2} \eta^1 \left[\frac{1}{2} \left(\bar{e} \gamma_\rho (1 - \gamma_5) \frac{1}{\not{q}} e^c \right) J_{V-A}^\rho J_{PS} \right. \\ &\quad \left. + \frac{1}{8} \left(\bar{e} \gamma_\rho (1 - \gamma_5) \frac{1}{\not{q}} \sigma_{\mu\nu} e^c \right) J_{V-A}^\rho J_T^{\mu\nu} \right], \end{aligned} \quad (\text{A.4})$$

where $J_{PS} = \bar{u}_y(1 + \gamma_5)d^y$ and $J_T^{\mu\nu} = \bar{u}_y\sigma^{\mu\nu}(1 + \gamma_5)d^y$ are the pseudo-scalar and tensor currents respectively. A Feynman diagram depicting this process is displayed in fig. 3. The matrix element is [4, 5]

$$M_{\lambda'_{113}\lambda'_{131}} = \eta^1 (M_{\tilde{q}}^{2N} + M_{\tilde{q}}^\pi), \quad (\text{A.5})$$

η^1 is defined as in eq. (A.3) with $n = 1$, and M^{2N} and M^π denote the 2 nucleon mode and pion mode contributions and will be detailed in Appendix B.

A.3 Sparticle exchange: $0\nu\beta\beta$ via $\lambda'_{111}\lambda'_{111}$

Following the notation of [1], the effective Lagrangian with λ'_{111} in the direct RPV $0\nu\beta\beta$ process involving exchange of two SUSY particles is given by

$$\begin{aligned} \mathcal{L}_{\lambda'_{111}\lambda'_{111}}^{eff, \Delta L_e=2}(x) &= \frac{G_F^2}{2} m_p^{-1} [\bar{e}(1 + \gamma_5)e^c] \\ &\quad \times \left[(\eta_{\tilde{g}} + \eta_\chi)(J_{PS}J_{PS} - \frac{1}{4}J_T^{\mu\nu}J_{T\mu\nu}) + (\eta_{\chi\tilde{e}} + \eta'_{\tilde{g}} + \eta_{\chi\tilde{f}})J_{PS}J_{PS} \right] \end{aligned} \quad (\text{A.6})$$

where the RPV coefficients are defined to be

$$\begin{aligned} \eta_{\tilde{g}} &= \frac{\pi\alpha_s}{6} \frac{\lambda'_{111}{}^2}{G_F^2} \frac{m_p}{m_{\tilde{g}}} \left(\frac{1}{m_{\tilde{u}_L}^4} + \frac{1}{m_{\tilde{d}_R}^4} - \frac{1}{2m_{\tilde{u}_L}^2 m_{\tilde{d}_R}^2} \right), \\ \eta_\chi &= \frac{\pi\alpha_2}{2} \frac{\lambda'_{111}{}^2}{G_F^2} \sum_{i=1}^4 \frac{m_p}{m_{\chi_i}} \left(\frac{\epsilon_{L_i}^2(u)}{m_{\tilde{u}_L}^4} + \frac{\epsilon_{R_i}^2(d)}{m_{\tilde{d}_R}^4} - \frac{\epsilon_{L_i}(u)\epsilon_{R_i}(d)}{m_{\tilde{u}_L}^2 m_{\tilde{d}_R}^2} \right), \\ \eta_{\chi\tilde{e}} &= 2\pi\alpha_2 \frac{\lambda'_{111}{}^2}{G_F^2} \sum_{i=1}^4 \frac{m_p}{m_{\chi_i}} \left(\frac{\epsilon_{L_i}^2(e)}{m_{\tilde{e}_L}^4} \right), \\ \eta'_{\tilde{g}} &= \frac{2\pi\alpha_s}{3} \frac{\lambda'_{111}{}^2}{G_F^2} \frac{m_p}{m_{\tilde{g}}} \left(\frac{1}{m_{\tilde{u}_L}^2 m_{\tilde{d}_R}^2} \right), \\ \eta_{\chi\tilde{f}} &= \pi\alpha_2 \frac{\lambda'_{111}{}^2}{G_F^2} \sum_{i=1}^4 \frac{m_p}{m_{\chi_i}} \left(\frac{\epsilon_{L_i}(u)\epsilon_{R_i}(d)}{m_{\tilde{u}_L}^2 m_{\tilde{d}_R}^2} - \frac{\epsilon_{L_i}(u)\epsilon_{L_i}(e)}{m_{\tilde{u}_L}^2 m_{\tilde{e}_L}^2} - \frac{\epsilon_{L_i}(e)\epsilon_{R_i}(d)}{m_{\tilde{e}_L}^2 m_{\tilde{d}_R}^2} \right), \end{aligned} \quad (\text{A.7})$$

and again we follow the notation of [1]. The ϵ 's denote rotations between mass and gauge eigenbasis in the gaugino-fermion-sfermion vertices. To facilitate comparisons with the literature, we display only the first generation sparticle contribution above but include contributions from all three generations in the numerical calculations. The relevant Feynman diagrams are displayed in fig. 4. Note that our expressions above are different from those presented in [1], [2] and [62]. Reference [1] made an approximation when extracting the colour singlet currents from the Feynman diagrams. Also, the expressions for η_χ and $\eta_{\chi\tilde{f}}$ (following the convention of [1]) are different, with the discrepancy coming from the colour flows of fig. 4(e) and fig. 4(f). References [2, 62] took proper account of the colour singlet extraction, which we have checked independently. However η_χ and $\eta_{\chi\tilde{f}}$ remained the same as in [1]. In the parameter space we explore, the numerical differences induced by such changes in the η s are small compared to the uncertainty in the nuclear matrix elements.

$M_{\lambda'_{111}}$ is given by [1, 2]

$$M_{\lambda'_{111}} = (\eta_{\tilde{g}} + \eta_\chi)M_{\tilde{g}}^{2N} + (\eta_{\chi\tilde{e}} + \eta'_{\tilde{g}} + \eta_{\chi\tilde{f}})M_{\tilde{f}}^{2N} + \frac{3}{8} \left((\eta_{\tilde{g}} + \eta_\chi) + \frac{5}{3}(\eta_{\tilde{g}} + \eta_\chi + \eta_{\chi\tilde{e}} + \eta'_{\tilde{g}} + \eta_{\chi\tilde{f}}) \right) \left(\frac{4}{3}M^{1\pi} + M^{2\pi} \right). \quad (\text{A.8})$$

The η s correspond to those defined in eq. (A.7), and $M_{\tilde{g},\tilde{f}}^{2N}$, $M^{1\pi}$ and $M^{2\pi}$ denote the 2 nucleon, 1 pion and 2 pion exchange modes respectively. They are detailed in Appendix B.

B. Nuclear Matrix Elements

channel	NME(^{76}Ge)	value	Ref.
$\lambda'_{111}\lambda'_{111}$	$M_{\tilde{g}}^{2N}$	283	[1]
	$M_{\tilde{f}}^{2N}$	13.2	[1]
	$M^{1\pi}$	-18.2	[2]
	$M^{2\pi}$	-601	[2]
$\lambda'_{113}\lambda'_{131}$	$M_{\tilde{q}}^{2N}$	-0.9	[5]
	$M_{\tilde{q}}^\pi$	604	[5]
$m_{\beta\beta}$	M_ν	2.8	[63]

Table 1: Nuclear matrix elements of ^{76}Ge used. The value of the 2 nucleon mode contribution to $M_{\lambda'_{113}\lambda'_{131}}$ includes a factor of $\frac{1}{2}$ discussed in footnote 1. For model details of the NME calculations, we refer readers to the literature.

As we are primarily interested in collider effects due to couplings from the direct contributions, we adopt numerical values collected from various sources in the literature for our discussions here. These parameters are displayed in table 1.

References

- [1] M. Hirsch, H. V. Klapdor-Kleingrothaus and S. G. Kovalenko, Phys. Rev. D **53**, 1329 (1996) [arXiv:hep-ph/9502385].

- [2] A. Faessler, S. Kovalenko and F. Simkovic, Phys. Rev. D **58** (1998) 115004 [arXiv:hep-ph/9803253].
- [3] M. Hirsch, H. V. Klapdor-Kleingrothaus and S. G. Kovalenko, Phys. Lett. B **372**, 181 (1996) [Erratum-ibid. B **381**, 488 (1996)] [arXiv:hep-ph/9512237].
- [4] H. Päs, M. Hirsch and H. V. Klapdor-Kleingrothaus, Phys. Lett. B **459**, 450 (1999) [arXiv:hep-ph/9810382];
- [5] A. Faessler, T. Gutsche, S. Kovalenko and F. Simkovic, arXiv:0710.3199 [hep-ph].
- [6] J. L. Goity and M. Sher, Phys. Lett. B **346** (1995) 69 [Erratum-ibid. B **385** (1996) 500] [arXiv:hep-ph/9412208].
- [7] G. R. Farrar and P. Fayet, Phys. Lett. B **76** (1978) 575.
- [8] N. Sakai and T. Yanagida, Nucl. Phys. B **197** (1982) 533.
- [9] S. Weinberg, Phys. Rev. D **26** (1982) 287.
- [10] L. E. Ibanez and G. G. Ross, Phys. Lett. B **260** (1991) 291.
- [11] H. K. Dreiner, C. Luhn and M. Thormeier, Phys. Rev. D **73** (2006) 075007 [arXiv:hep-ph/0512163].
- [12] L. E. Ibanez and G. G. Ross, Nucl. Phys. B **368** (1992) 3.
- [13] H. K. Dreiner, J. Soo Kim and M. Thormeier, arXiv:0711.4315 [hep-ph].
- [14] W. Buchmuller, L. Covi, K. Hamaguchi, A. Ibarra and T. Yanagida, JHEP **0703** (2007) 037 [arXiv:hep-ph/0702184].
- [15] A. de Gouvea and J. Jenkins, Phys. Rev. D **77** (2008) 013008 [arXiv:0708.1344 [hep-ph]].
- [16] B. C. Allanach, Comput. Phys. Commun. **143** (2002) 305 [arXiv:hep-ph/0104145].
- [17] A. S. Joshipura and M. Nowakowski, Phys. Rev. D **51** (1995) 2421 [arXiv:hep-ph/9408224].
- [18] M. Nowakowski and A. Pilaftsis, Nucl. Phys. B **461** (1996) 19 [arXiv:hep-ph/9508271].
- [19] Y. Grossman and H. E. Haber, Phys. Rev. Lett. **78** (1997) 3438 [arXiv:hep-ph/9702421].
- [20] Y. Grossman and H. E. Haber, Phys. Rev. D **59** (1999) 093008 [arXiv:hep-ph/9810536].
- [21] A. S. Joshipura and S. K. Vempati, Phys. Rev. D **60** (1999) 111303 [arXiv:hep-ph/9903435].
- [22] S. Davidson and M. Losada, JHEP **0005** (2000) 021 [arXiv:hep-ph/0005080].
- [23] S. Davidson and M. Losada, Phys. Rev. D **65** (2002) 075025 [arXiv:hep-ph/0010325].
- [24] Y. Grossman and S. Rakshit, Phys. Rev. D **69** (2004) 093002 [arXiv:hep-ph/0311310].
- [25] A. Dedes, S. Rimmer and J. Rosiek, JHEP **0608**, 005 (2006) [arXiv:hep-ph/0603225].
- [26] B. C. Allanach, C. H. Kom and H. Päs, arXiv:0902.4697 [hep-ph].
- [27] F. Deppisch and H. Päs, Phys. Rev. Lett. **98** (2007) 232501 [arXiv:hep-ph/0612165].
- [28] V. M. Gehman and S. R. Elliott, J. Phys. G **34**, 667 (2007) [Erratum-ibid. **G35**, 029701 (2008)] [arXiv:hep-ph/0701099].
- [29] D. Aristizabal Sierra, M. Hirsch and S. G. Kovalenko, Phys. Rev. D **77** (2008) 055011 [arXiv:0710.5699 [hep-ph]].

- [30] A. Wodecki, W. A. Kaminski and F. Simkovic, Phys. Rev. D **60** (1999) 115007 [arXiv:hep-ph/9902453].
- [31] S. Rakshit, G. Bhattacharyya and A. Raychaudhuri, Phys. Rev. D **59** (1999) 091701 [arXiv:hep-ph/9811500].
- [32] A. Abada and M. Losada, Phys. Lett. B **492** (2000) 310 [arXiv:hep-ph/0007041].
- [33] A. Abada, G. Bhattacharyya and M. Losada, Phys. Rev. D **66** (2002) 071701 [arXiv:hep-ph/0208009].
- [34] M. Hirsch, M. A. Diaz, W. Porod, J. C. Romao and J. W. F. Valle, Phys. Rev. D **62** (2000) 113008 [Erratum-ibid. D **65** (2002) 119901] [arXiv:hep-ph/0004115].
- [35] M. A. Diaz, M. Hirsch, W. Porod, J. C. Romao and J. W. F. Valle, Phys. Rev. D **68** (2003) 013009 [Erratum-ibid. D **71** (2005) 059904] [arXiv:hep-ph/0302021].
- [36] B. C. Allanach and C. H. Kom, JHEP **0804** (2008) 081 arXiv:0712.0852 [hep-ph].
- [37] M. Misiak, S. Pokorski and J. Rosiek, Adv. Ser. Direct. High Energy Phys. **15** (1998) 795 [arXiv:hep-ph/9703442].
- [38] D. Choudhury and P. Roy, Phys. Lett. B **378** (1996) 153 [arXiv:hep-ph/9603363].
- [39] M. Hirsch, J. C. Romao and J. W. F. Valle, Phys. Lett. B **486**, 255 (2000) [arXiv:hep-ph/0002264].
- [40] L. Baudis *et al.*, Phys. Rev. Lett. **83** (1999) 41 [arXiv:hep-ex/9902014].
- [41] H. V. Klapdor-Kleingrothaus *et al.*, Eur. Phys. J. A **12**, 147 (2001) [arXiv:hep-ph/0103062].
- [42] C. Amsler *et al.* [Particle Data Group], Phys. Lett. B **667** (2008) 1.
- [43] G. Pantis, F. Simkovic, J. D. Vergados and A. Faessler, Phys. Rev. C **53** (1996) 695 [arXiv:nucl-th/9612036].
- [44] S. Schael, and others, Eur. Phys. J. C **47** (2006) 547-587 [arXiv:hep-ex/0602042].
- [45] O. Deschamps, arXiv:0810.3139 [hep-ph].
- [46] H. K. Dreiner, P. Richardson and M. H. Seymour, Phys. Rev. D **63** (2001) 055008 [arXiv:hep-ph/0007228].
- [47] J. L. Hewett and T. G. Rizzo, arXiv:hep-ph/9809525.
- [48] J. Kalinowski, R. Rückl, H. Spiesberger and P. M. Zerwas, Phys. Lett. B **414** (1997) 297 [arXiv:hep-ph/9708272].
- [49] B. Allanach *et al.* [R parity Working Group Collaboration], arXiv:hep-ph/9906224.
- [50] H. K. Dreiner, P. Richardson and M. H. Seymour, JHEP **0004** (2000) 008 [arXiv:hep-ph/9912407].
- [51] S. Dimopoulos, R. Esmailzadeh, L. J. Hall and G. D. Starkman, Phys. Rev. D **41** (1990) 2099.
- [52] H. K. Dreiner, M. Guchait and D. P. Roy, Phys. Rev. D **49**, 3270 (1994) [arXiv:hep-ph/9310291].
- [53] S. Kolb, M. Hirsch, H. V. Klapdor-Kleingrothaus and O. Panella, Phys. Rev. D **64**, 115006 (2001) [arXiv:hep-ph/0102175].
- [54] T. Han and B. Zhang, Phys. Rev. Lett. **97**, 171804 (2006) [arXiv:hep-ph/0604064].

- [55] S. Kolb, M. Hirsch, H.V. Klapdor-Kleingrothaus, O. Panella, Phys. Rev. **D64** (2001) 115006 [arXiv:hep-ph/0102175]
- [56] H. K. Dreiner, S. Grab and M. K. Trenkel, arXiv:0808.3079 [hep-ph].
- [57] F. T. . Avignone, S. R. Elliott and J. Engel, Rev. Mod. Phys. **80** (2008) 481 [arXiv:0708.1033 [nucl-ex]].
- [58] C. Aalseth *et al.*, arXiv:hep-ph/0412300.
- [59] K. S. Babu and R. N. Mohapatra, Phys. Rev. Lett. **75** (1995) 2276 [arXiv:hep-ph/9506354].
- [60] B. Pontecorvo, Sov. Phys. JETP **26** (1968) 984 [Zh. Eksp. Teor. Fiz. **53** (1967) 1717].
- [61] Z. Maki, M. Nakagawa and S. Sakata, Prog. Theor. Phys. **28** (1962) 870.
- [62] A. Faessler and F. Simkovic, J. Phys. G **24** (1998) 2139 [arXiv:hep-ph/9901215].
- [63] F. Simkovic, G. Pantis, J. D. Vergados and A. Faessler, Phys. Rev. C **60** (1999) 055502 [arXiv:hep-ph/9905509].
- [64] S. R. Elliott and J. Engel, J. Phys. G **30** (2004) R183 [arXiv:hep-ph/0405078].
- [65] V. A. Rodin, A. Faessler, F. Simkovic and P. Vogel, Nucl. Phys. A **766**, 107 (2006) [Erratum-ibid. A **793**, 213 (2007)] [arXiv:0706.4304 [nucl-th]].
- [66] J. Charles, Talk at Anapri, Capri island, June 16th 2008
http://ckmfitter.in2p3.fr/plots_Summer2008/